USE OF X-RAY COMPUTER TOMOGRAPHIC IMAGERY IN LOCATION OF TARGET FRACTURES AND PROJECTILE FRAGMENTS AROUND LABORATORY HYPERVELOCITY IMPACT CRATERS.

A. T. Kearsley[1], M. J. Burchell[2], R. Abell[1] and M. J. Cole[2]. [1]IARC, Department of Mineralogy, Natural History Museum, London, SW7 5BD, UK, (antk@nhm.ac.uk), [2]School of Physical Science, University of Kent, Canterbury, CT2 7NH, UK,

Introduction: Fracture development is an important process in hypervelocity impact cratering on brittle targets of every scale from micrometers to 100s of kilometers. Careful mapping and orientation of structures visible at the surface may allow interpretation of cratering mechanisms e.g. [1], especially those related to formation and late stage modification of much larger craters. However, large scale structural trend information available from down-well sensing or cores from deep-drilling is unfortunately limited, and fine-scale interpretation of seismic data returned from beneath highly fragmented crater infill is very difficult.

Analysis of melt at impact craters may reveal the type of bolide [2], although discovery of (modified) cm scale solid chondritic fragments [3] in melt of high meteoritic content at the Morokweng crater [4], and the complex behaviour of iron projectiles in laboratory impacts [5] highlight limitations in current understanding of projectile processing during impact. Signatures of bolide components have also been found in fractures containing breccia and impact melt e.g. [6-8], usually as distinctive minor- and trace-element and extraterrestrial isotope signatures within bulk rock, rather than as discrete impactor fragments. Projectile residue occurs in fractures around sub-mm craters formed by micrometeoroid impact on brittle surfaces of spacecraft in low Earth orbit, and also in experimental mm scale impacts of metal onto rock [9].

Mechanisms of impact-driven fracturing have been studied by a number of authors, e.g. [10] who used tensile and fracture strengths determined in laboratory experiments to model fracturing at Barringer Crater [6]. Direct, true-scale comparisons between numerical simulations and experimental impacts can include realistic brittle fracturing, and it is therefore worthwhile to document target subsurface structure in detail. Cut sections have been used to show fractures in a number of studies e.g. [5, 10]. In this paper we show the results of testing high-resolution X-ray Computed micro-Tomographic imaging (micro-CT) [11] in locating three dimensional sub-surface fractures and impactor residue in laboratory impacts at cm scale.

Experimental methods: Targets for preliminary study were cast blocks of transparent silicone polymer, density ~2.3 gcm^{-3}, in which optical imagery could verify CT reconstructions. Projectiles were spheres of Cu (1 mm) and stainless steel (2 mm), fired at ~5 kms^{-1} in the two-stage light gas gun at the University of Kent. Impacted targets were photographed, and imaged in the X-Tek HMX-ST CT system at the Natural History Museum. A range of electron gun accelerating voltages were used (typically 180 kV), onto tungsten which generated 50-70 keV X-rays, filtered through a 1 mm Cu foil to reduce X-ray background. The Perkin-Elmer detector captured images at 720 rotation points, each accumulated for 1 second. Tomographic reconstructions with fine voxel size (40 µm) were then computed for specific subsets of transmission intensity, representing solid polymer, open fractures and projectile remnants.

Subsurface Fracturing: Targets showed extensive damage, with spallation of the surface in roughly triangular shards, bounded by subvertical radial fractures and low angle basal fractures. The melt-lined pit, marking the location of the transient crater, was lost by extensive spallation due to relatively deep penetration resulting from strong density contrast between projectile and target. Nevertheless, melt-pit dimensions can be inferred as ~1 mm diameter. Below the surface, both optical and CT images reveal a complex suite of intersecting fractures (Figures 1, 2 and 3).

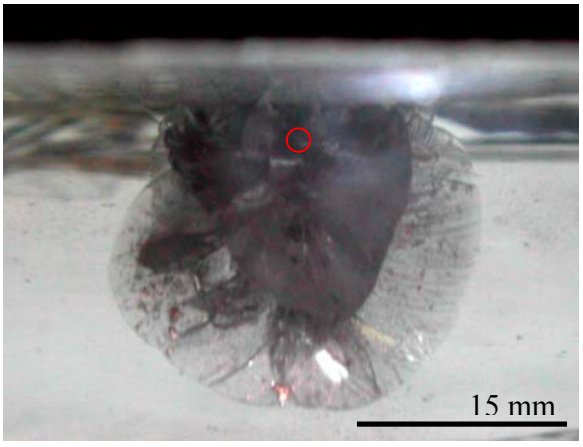

Figure 1. Side view optical image of structure below surface of block, created by impact of 1 mm Cu sphere from above. Approximate position of spalled crater melt pit shown in red. Note the extensive inclined sub-radial fractures, and fragments of reflective Cu projectile, to ~18 mm depth and ~12.5 mm radius.

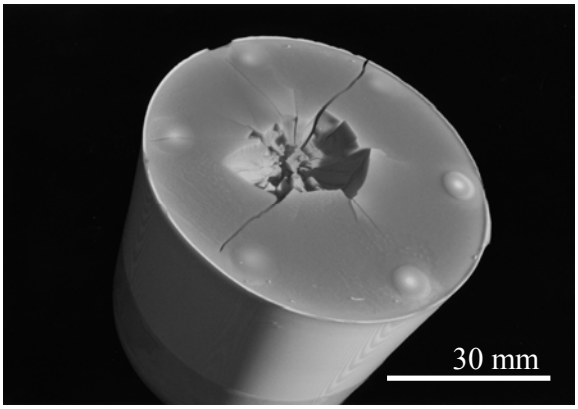

Figure 2. CT reconstruction of target surface viewed from above/oblique. Stainless steel projectile, 2mm diameter, shot G160606#1. Note extensive spall detachment of segments bounded by radial fractures.

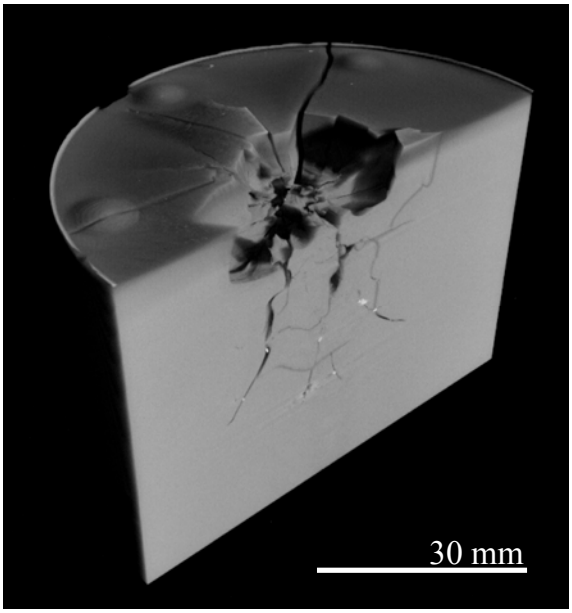

Figure 3. Cutaway vertical section in CT reconstruction, showing fracture system extending to >> 10 times melt pit dimensions, shot G160606#1.

Projectile fragment distribution.: Irregular shrapnel, up to mm size, were found scattered along the full extent of the fracture systems (Figure 4).

Discussion: X-ray micro-CT clearly shows great potential for visualization of fracturing and projectile debris location. Our first target samples have proven ideal for testing CT technique on material of similar density to many rocks, but we do not yet have an adequate equation of state for the polymer to enable numerical modeling of impact fracture development.

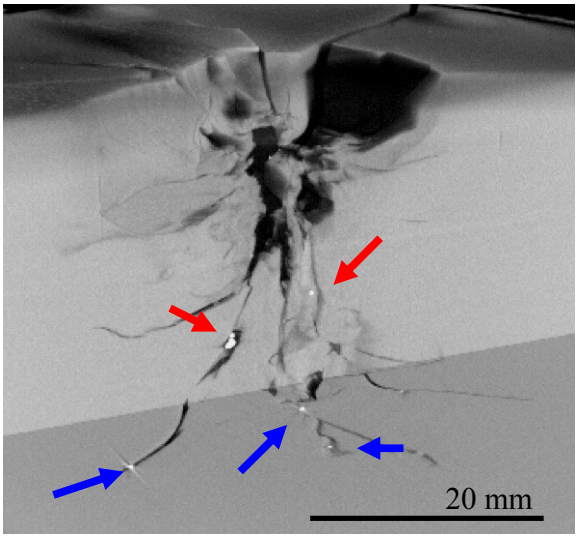

Figure 4. CT cutaway, showing steel projectile fragments (bright) in the fracture system below impact structure, shot G160606#1. Red arrows denote location of fragments in vertical section, blue horizontal.

We are currently examining an impacted block target of a porous sandstone, which shows a well-defined (albeit irregular) melt pit, and a surrounding zone of shallow conchoidal spallation, with melt-lined surfaces that display abundant droplets of impactor metal composition. We shall use micro-CT to determine the extent of sub-surface fracturing and deposition of projectile-derived residue in this sample. Our next experiment will impact a meteoritic kamacite grain onto a target of laminated mylonitic garnet gneiss, from which we aim to document both projectile emplacement and compositional fractionation in ejecta.

Acknowledgements: We wish to thank the staff of X-Tek for their assistance in the acquisition and processing of our CT reconstructions.

References: [1] Kenkmann T et al. (2005) *GSA Spec. Paper, 384,* 85-115. [2] Koeberl C (2002) *Min. Mag., 66,* 745-768. [3] Maier W D et al. (2006) *Nature, 441,* 203-206. [4] Koeberl C and Reimold W U (2003) *Geochim. et Cosmochim. Acta, 67,* 1837–1862. [5] Kenkmann T et al. (2007) *LPS XXXVIII,* Abstract #1831. [6] Kring D A (2007) *Guidebook to the Geology of Barringer Meteorite Crater, Arizona (a.k.a. Meteor Crater). LPI Cont. 1355*. [7] El Goresy A and Chao E C T (1976). *EPSL, 31*, 330-340. [8] Koeberl C et al. (1996) *Geology, 24*, 913-916. [9] Kearsley A T et al. (2004) *Meteoritics and Planetary Sci., 39,* 247-265. [10] Ai H-A and Ahrens T J (2004) *Meteoritics and Planetary Sci., 39,* 233-246. [11] Koeberl C et al. (2002) *JGR, 107,* 1-9.